Protein Cell 2011, 2(12): 1006–1013
DOI 10.1007/s13238-011-1121-3

Protein & Cell

RESEARCH ARTICLE

Engineering a zinc binding site into the *de novo* designed protein DS119 with a βαβ structure

Cheng Zhu[1*], Changsheng Zhang[1*], Huanhuan Liang[1,3], Luhua Lai[1,2] ✉

[1] Beijing National Laboratory for Molecular Sciences, State Key Laboratory for Structural Chemistry of Unstable and Stable Species, College of Chemistry and Molecular Engineering, Peking University, Beijing 100871, China
[2] Center for Theoretical Biology, Peking University, Beijing 100871, China
[3] Present address: National Laboratory of Biomacromolecules, Institute of Biophysics, Chinese Academy of Sciences, Beijing 100101, China
✉ Correspondence: lhlai@pku.edu.cn
Received November 7, 2011 Accepted November 21, 2011

ABSTRACT

Functional proteins designed *de novo* have potential application in chemical engineering, agriculture and healthcare. Metal binding sites are commonly used to incorporate functions. Based on a *de novo* designed protein DS119 with a βαβ structure, we have computationally engineered zinc binding sites into it using a home-made searching program. Seven out of the eight designed sequences tested were shown to bind Zn^{2+} with micromolar affinity, and one of them bound Zn^{2+} with 1:1 stoichiometry. This is the first time that metalloproteins with an α, β mixed structure have been designed from scratch.

KEYWORDS βαβ, *de novo*, design, folding, zinc-binding

INTRODUCTION

The important goal of protein design is to explore relationships between protein structures and functions. Various approaches can be used to incorporate functions in the designed protein scaffolds (Smith and Hecht, 2011), and metal binding sites have been a particularly interesting target for this purpose because the biological chemistry of metals is extremely rich (Holm et al., 1996; Lu et al., 2009). For example, by engineering different cofactors like Zn^{2+} (Handel et al., 1993), Fe^{2+}/Fe^{3+} (Kaplan and DeGrado, 2004), heme (Choma et al., 1994) and abiological chromophore (DPP) Zn (Fry et al., 2010) into the *de novo* designed four-helix bundles, functions like phenol oxidation, electron transfer, and non-linear optical properties have been obtained.

Zinc binding sites are of special importance for both structural and functional reasons, as in zinc fingers (Berg and Shi, 1996), carbonic anhydrase (Christianson and Fierke, 1996), and zinc metalloproteases (Meinnel et al., 1996). Using rational design and *in vitro* evolution, researchers have introduced zinc binding sites into different protein structures such as four-helix bundles (Regan and Clarke, 1990), antibody light chain (Wade et al., 1993), triple-strand coiled-coil (Kiyokawa et al., 2004), and retinal binding protein (Muller and Skerra, 1994). Recently, zinc binding proteins have been engineered for more sophisticated tasks, for example, protein conformation switches (Cerasoli et al., 2005; Ambroggio and Kuhlman, 2006), biosensors (Shults et al., 2003), purification tags (Pasquinelli et al., 2000), control of oligomerization states (Phillips et al., 2010), catalytic zinc sites (Nomura and Sugiura, 2004), or even regulating a bacterial signal transduction pathway (Dwyer et al., 2003). And zinc fingers combined with restriction endonucleases or recominases have emerged as an important tool for molecular biology for their application in editing genomes (Miller et al., 2007; Wu et al., 2007; Proudfoot et al., 2011). So the functions of zinc binding sites are widely explored in designed proteins.

To establish a valid and simple method for engineering zinc binding sites, we chose a designed small protein DS119 as the scaffold to incorporate zinc ions and developed a computational approach. DS119 was a *de novo* designed protein with a unique βαβ structure (Liang et al., 2009). It is highly thermally stable and folds quickly into a monomeric structure, providing an attractive target for functional

[*] These authors contributed equally to the work.

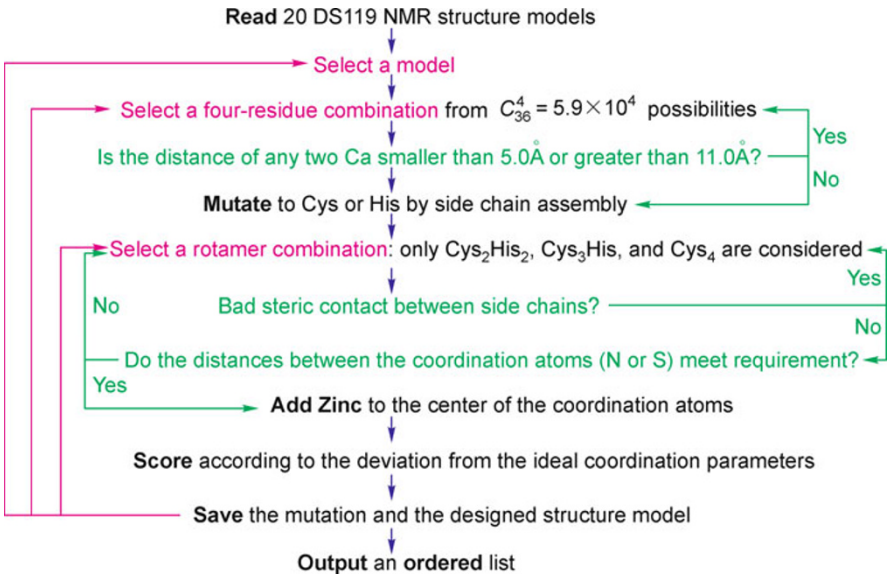

Figure 1. Computational process for identifying zinc binding sites in DS119.

engineering. Similar to the ββα zinc finger structure, the βαβ motif also contains one α-helix and two β strands, though the two β strands are parallel compared to the anti-parallel β structure in zinc fingers. Zinc finger structures are commonly used in DNA binding proteins, which have inducible structure by binding to zinc ions. In the present study, we explored the possibility of introducing a zinc binding site into DS119 and studied the influence of the zinc binding on its structure and folding properties.

RESULTS

Twenty NMR structure models of DS119 (PDB code: 2KI0) which embody the backbone flexibility were used as scaffolds to identify potential zinc binding sites. This approach is different from previous metalloprotein design programs which only search in one rigid conformation (Hellinga and Richards, 1991; Clarke and Yuan, 1995). Three types of zinc coordination sites were considered: Cys_4, Cys_3His and Cys_2His_2, and their ideal coordination parameters were obtained by statistical analysis of natural zinc binding proteins in the Protein Data Bank (Berman et al., 2000). The average values are as follows: S-Zn bond length is 2.32 Å, N-Zn bond length is 2.09 Å, C_β-S-Zn angle is 107.3°, C_γ-N_δ-Zn or C_ε-N_ε-Zn angle is 128.4°, C_α-C_β-S-Zn dihedral angle can have three values: 111.1°, 184.4° and 269.4°, C_γ-C_ε-Zn-N_δ or C_δ-C_ε-Zn-Nε is coplanar (Table S1). The computational process of identifying zinc binding sites consisted of three steps (Fig. 1). First, for each conformational scaffold the residues were substituted by Cys and His using the basic rotamer library of DeMaeyer et al. (1997), and the substitutions with steric contact were pruned. Next all the four-site combinations, in which the Cα distances between any two residues were in the range of 11.0–5.0 Å, and were carefully examined to determine whether they could accommodate the Cys_4, Cys_3His or Cys_2His_2 binding coordination. The examination used several rules: (1) Zn^{2+} was placed on the center of four coordination atoms, (2) the coordination structure was scored according to its deviation from ideal parameters (see supplementary material), and (3) the structure models were ranked by the score. Finally the models with similar sequences were clustered and 20 different design modes (Table S2) were obtained.

According to the top-scoring solutions, eight DS119 mutants (called BABZ) were expressed, purified and tested for their zinc binding affinities and structural properties (Table 1 and Fig. 2). Isothermal titration calorimetry (ITC) was used to check for possible Zn^{2+}-protein interactions, and seven out of eight BABZ proteins were shown to bind Zn^{2+} with a medium tendency. Their dissociation constants (K_d) were in the range of 2–20 μmol/L (Table 2). Based on the ITC results, BABZ5 was chosen for further investigation as the titration curve indicated it bound Zn^{2+} with 1:1 stoichiometry (Fig. 3B). BABZ5 was designed to bind Zn^{2+} with two N-terminal His, one Cys on the helix, and another Cys on the β strand. It showed good secondary structure on CD, preserving the βαβ fold of DS119 (Table 2 and Fig. 3C). In gel filtration chromatography the peak of BABZ5 without Zn^{2+} shifted towards the aggregation state, and upon adding Zn^{2+} in the running buffer it moved to the monomer position (Table 2 and Fig. 3D). The peak of BABZ5 also showed trailing edge boundary and expansion towards the monomer state. We thought this was due to the equilibrium between the bound and unbound state, since the binding affinity of BABZ5

Table 1 Sequences of DS119 and BABZ proteins

DS119	GSGQV RTIWV GGTPE ELKKL KEEAK KANIR VTFWG D
BABZ1	GSGQV HTIWV GGTPE ELKKL KECAK KANCR HTFWG D
BABZ2	GSGHC RTIWV GGTPE ELKKL KEEAK KAHCR VTFWG D
BABZ3	GSGHV HTIWV GGTPE ELKKL KEEAK KCNCR VTFWG D
BABZ4	GSGCC RTIWV GGTPE ELKKL KEEAK KHNCR VTFWG D
BABZ5	GSGHV HTIWV GGTPE ELKKL KECAK KANCR VTFWG D
BABZ6	GSGHV CTIWV GGTPE ELKKL KEHAK KANCR VTFWG D
BABZ7	GSGQV RTIWC GGTPE ECKKC KEEAK KANIR VTHWG D
BABZ8	GSGQV RTHWV GGTPE ELKKC KEEAK KANCR CTFWG D

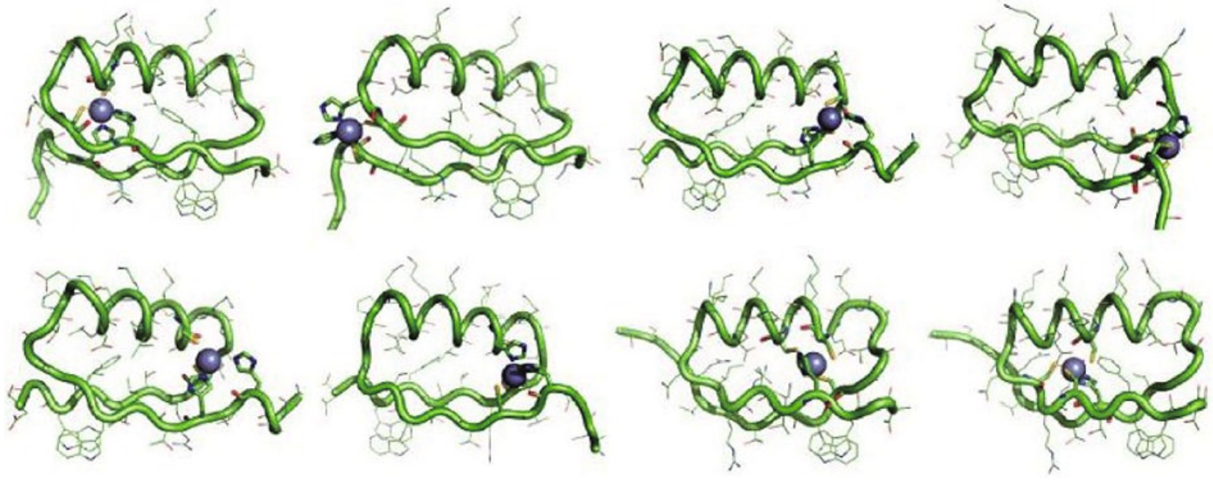

Figure 2. Structure models of BABZ proteins. Upper row from left to right: BABZ1, 2, 3 and 4, lower row: BABZ5, 6, 7 and 8. Zn^{2+} is indicated as a silver sphere, and coordination residues (histidine or cysteine) are shown as sticks.

Table 2 CD, gel filtration and ITC results of BABZ proteins

	BABZ1	BABZ2	BABZ3	BABZ4	BABZ5	BZBZ6	BZBZ7	BZBZ8
Aggregation state without Zn^{2+}	1.41	0.86	0.90	0.89	1.24	NA	1.42	1.40
Aggregation state with Zn^{2+}	1.41	NA[a]	NA	NA	1.03	NA	1.41	1.40
Secondary structures without Zn^{2+} (%)	42	91	92	99	98	94	43	34
Secondary structures with Zn^{2+}(%)	40	91	95	100	98	63	45	32
N[b]	0.65	0.51	NA[c]	0.55	0.93	0.40	0.40	0.72
K_d (μmol/L)	22	15	NA	7.5	2.2	8.8	4.5	2.3

[a] NA means no elution peak was observed in gel filtration.

[b] N is the molar ratio indicating how many Zn^{2+} ions interacted with one protein.

[c] NA means the interaction of BABZ3 and Zn^{2+} is too weak to be measured by ITC.

for Zn^{2+} was not extremely high (K_d was 2.2 μmol/L). The trailing edge is the result of a systematic increase in the migration rate across the advancing boundary, which in turn, is due to rapid self-association equilibrium. This phenomenon has been used in large-zone chromatography to determine the association constants (Stevens, 1986; Winzor, 2003).

There was no significant difference between the secondary structures of BABZ5 with and without Zn^{2+}, as indicated by CD in the far-UV region (Fig. 3C). However, their thermodynamics showed dramatic differences (Fig. 4). The CD signal at 222 nm was used to monitor the unfolding and refolding process of BABZ5. In the absence of Zn^{2+}, partially unfolded BABZ5 could not fold back to its original thermodynamic state, as indicated by the differences between its unfolding and refolding curves. After BABZ5 binds to Zn^{2+}, these two curves were identical, indicating the guiding role of Zn^{2+} during its folding process. Thus, BABZ5 binding with Zn^{2+} facilitated smooth transition from the unfolded state to the folded state.

Other BABZ proteins, which also showed zinc binding

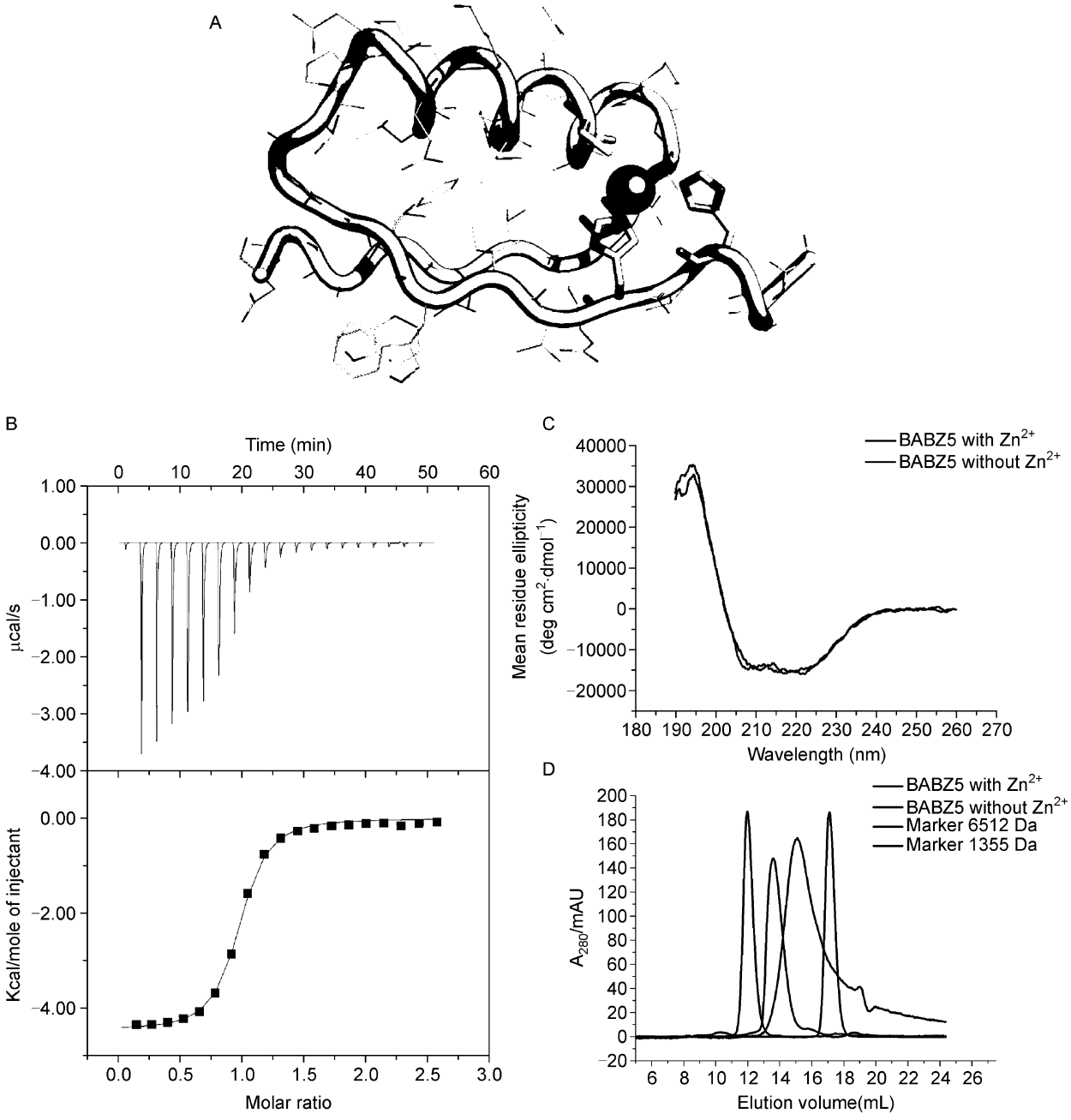

Figure 3. Structural and Zn^{2+}-binding properties of the designed BABZ5 protein. (A) Structure model of BABZ5 protein. Zn^{2+} is indicated as a silver sphere, and coordination residues (histidine or cysteine) are shown as sticks. (B) ITC measurement of BABZ5 and Zn^{2+} interactions. (C) CD spectra of BABZ5 with and without Zn^{2+}: BABZ5 in $ZnSO_4$ buffer (20 mmol/L Tris-HCl pH 7.3, 2 mmol/L $ZnSO_4$ and 100 µmol/L TCEP) (—), BABZ5 in EDTA buffer (20 mmol/L Tris-HCl pH 7.3, 1 mmol/L EDTA and 100 µmol/L TCEP) (—). (D) Gel filtration analysis of BABZ5 with and without Zn^{2+} using the same buffer as in CD, but adding 100 mmol/L NaCl. ITC, isothermal titration calorimetry.

affinities, falls mainly into two categories: BABZ2 and BABZ4 preserved the βαβ fold, and BABZ1, BABZ7 and BABZ8 were unstructured (Fig. 5). For the unstructured BABZ proteins, zinc-binding changed neither their secondary structure nor aggregation states. For BABZ2 and BABZ4, the molar ratios for the interactions between BABZ proteins and Zn^{2+} were not 1:1 as designed, according to ITC (Fig. S3). Since their coordination residues are located on flexible N-terminals, it is possible that the coordination sites were composed of residues from two monomeric proteins and the binding of

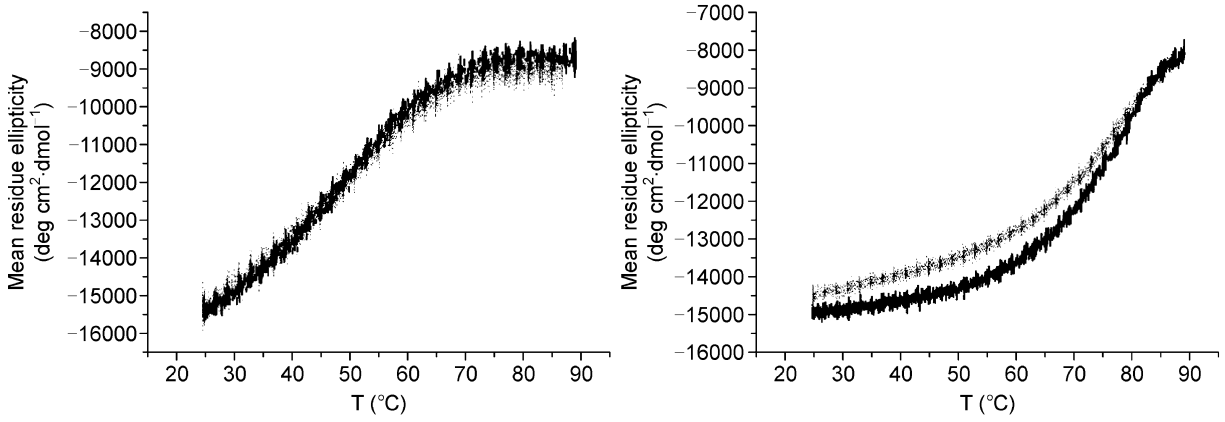

Figure 4. Thermal denaturation curves of BABZ5 with and without Zn^{2+}. Left: BABZ5 in $ZnSO_4$ buffer. Right: BABZ5 in EDTA buffer. Thermal unfolding was measured from 25°C to 90°C (—), and refolding was measured from 90°C to 25°C (—). CD signals at 222 nm were monitored.

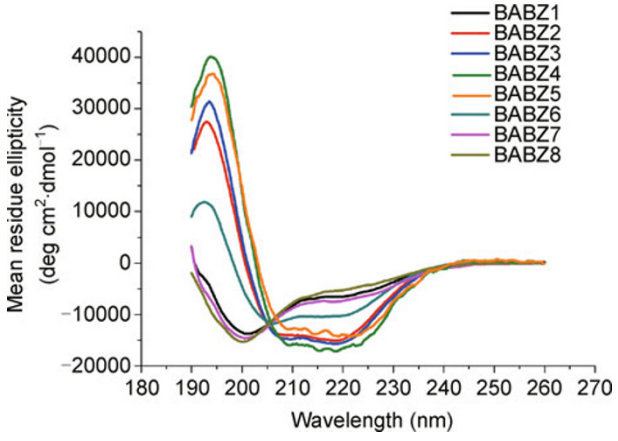

Figure 5. CD spectra of BABZ proteins with Zn^{2+}. Experiments were carried out in 20 mmol/L Tris-HCl buffer (pH 7.3) containing 2 mmol/L $ZnSO_4$ and 100 μmol/L TCEP.

Zn^{2+} could induce their oligomerization. So compared to BABZ5, they cannot be regarded as successful designs.

DISCUSSION

Although nature has used zinc fingers with ββα structure to incorporate Zn^{2+}, the βαβ motif with the same number of secondary structure elements has never been observed for this function. By using the previously designed DS119, we engineered zinc binding proteins with a βαβ structure. Compared to the binding induced folding process of zinc fingers, the conformation changes of BABZ5 after binding Zn^{2+} were not significant, partly due to the highly thermally stable structure of DS119 (Liang et al., 2009). It is challenging to design functional sites in a small *de novo* designed protein, and during the process of zinc binding sites engineering, much can be learned about its sequence, structure and folding relationship.

In order to engineer a zinc binding site in DS119, two to four mutations must be made. Which residues should be replaced is vital for a successful design. For example, BABZ1 resembled the most perfect tetrahedral coordination sites among all design modes, but the His_2/Cys_2 mutations damaged the protein structure, and binding to Zn^{2+} could not recover the βαβ fold. Similarly, in BABZ7 and BABZ8, the mutations essentially destroyed the hydrophobic core. So the overall folding involves a delicate interplay of hydrophobic packing, hydrogen bonding, and metal binding (Li et al., 2007, 2008). In addition, if the coordination residues are located on flexible terminals or loops, as in BABZ2 and BABZ4, zinc binding-induced aggregation may occur, especially for the small protein like βαβ, so the entropy cost to fix the coordination residues at specific conformations should be considered, as zinc binding in proteins is an entropy-driven process (Reddi et al., 2007). It has been demonstrated that the primary interactions are enough to produce potentially useful zinc binding affinity (Wade et al., 1993), and this agrees with our design work.

It is worth noting that the T_m value for the unfolding process of BABZ5 with Zn^{2+} was clearly lower than that without Zn^{2+}, which indicates zinc-binding stabilizes the unfolded state more than it does to the folded state. The unfolded state is hard to be considered apparently and is not included in our computational program. Nonetheless this phenomenon provides opportunities to study the folding mechanism of the βαβ motif, since the T_m values were reduced to a reasonable range (about 50°C) compared to DS119 (above 80°C), and the unfolding process is cooperative, which makes it more suitable for fast kinetic experiments like laser induced T-jump (Dyer et al., 1998).

Different methods have emerged for engineering novel

metalloproteins. The simplest way is to analyze protein scaffolds empirically and introduce cysteine-rich coordination sites. Several α-helical coiled-coil metalloproteins capable of binding Co(II), Fe(II), Zn(II), Cd(II), Hg(II), and As(II) have been designed this way (Matzapetakis et al., 2002; Petros et al., 2006). More complex coordination sites were engineered with the aid of computational searching, for example, the Cys_2-His_2 zinc binding sites and Fe_4-S_4 sites (Lu et al., 2001). Retrostructural analysis for designing diiron binding protein is the most complex approach by far (Lombardi et al., 2000). The natural diiron binding site was analyzed first to obtain the desired chelation geometry, the symmetry of the structure, and other rules for forming the binding site. Then the design was accomplished in a hierarchical manner: coordinated side chains were placed first, the residues for coordination stabilization and hydrophobic core came next, and last the polar residues and loops were fixed. Backbone conformation variation was considered in this computation process. Our work of designing zinc-binding βαβ small proteins shares some characteristics with the third method.

In conclusion, we have successfully engineered a zinc binding site in the *de novo* designed protein with a βαβ structure. The small zinc binding proteins provide valuable targets for protein folding research, and can be further engineered to target DNA sequences, or catalyze chemical reactions. This work provides an approach to engineering functional proteins with more complex structures.

MATERIALS AND METHODS

Cloning, protein expression and purification

The genes encoding BABZ proteins were synthesized by Invitrogen (Beijing, CN) and cloned into $pGEX_{4T-1}$ vectors (GE Healthcare). The proteins were expressed in *Escherichia coli* Rosetta cells for 6 h at 30°C and purified using standard GST-fusion proteins purification protocols. Using PBS (100 mmol/L NaCl, 40 mmol/L Na_2HPO_4/NaH_2PO_4 pH 7.3) containing 2 mmol/L DTT as running buffer and 10 mmol/L glutathione in Tris-HCl pH 8.0 as elution buffer, solutions containing the GST-fusion BABZ proteins were collected, and thrombin (Sigma) was added at 4°C to remove the N-terminal GST protein.

The samples containing BABZ proteins, glutathione, and thrombin were loaded onto an Agilent Zorbax 300SB-C18 column and purified by reversed-phase HPLC. Gradient-elution using water and acetonitrile was performed on the Agilent 1100 series HPLC. The peak corresponding to BABZ proteins was eluted at 45%–50% acetonitrile, and then collected for lyophilization. The purity of each protein sample was verified by high resolution mass spectrometry (Fourier Transform Ion Cyclotron Resonance Mass Spectrometer, Bruker APEX IV, USA).

Circular Dichroism

Circular Dichroism spectra (CD) were measured on a MOS 450 AF/CD (Biologic, France) at room temperature, using 1 mm quartz cuvettes for the far-UV region (190 nm to 250 nm). Band width and scan speed were set as 0.5 nm and 100 nm/min. Protein samples were dissolved to a final concentration of 0.2 mg/mL in 20 mmol/L Tris-HCl buffer (pH 7.3) containing 2 mmol/L $ZnSO_4$ or 1 mmol/L EDTA, and 100 μmol/L TCEP.

The secondary structure content was calculated using DS119 as standard. The normalized CD signal of DS119 at 222 nm was −15,410 deg $cm^2 \cdot dmol^{-1}$and this value was set as 100%. The CD signal of BABZ proteins at 222 nm divided by −15,410 deg $cm^2 \cdot dmol^{-1}$ gave their secondary structure content.

Thermal denaturation curves of BABZ proteins were also obtained on the MOS 450 AF/CD using the Peltier accessory with 10 mm quartz cuvettes. The CD signal at 222 nm was recorded. The protein concentration was 0.02 mg/mL in the same buffers as in far-UV CD, and heating was performed at 1°C/min speed from 25°C to 90°C.

Gel filtration chromatography

Protein samples were dissolved in 20 mmol/L Tris-HCl buffers (pH 7.3) containing 2 mmol/L $ZnSO_4$ or 1 mmol/L EDTA, and 100 mmol/L NaCl to final concentrations of 50 μmol/L, and then loaded onto a Superdex^{TM} Peptide 10/300 GL column (GE Healthcare). The column was eluted using the same buffer with a flow rate of 0.4 mL/min and UV absorption at 280 nm was monitored.

The molecular markers are cytochrome C (12.4 kDa), aprotinin (6512 Da), and vitamin B12 (1355 Da). The lg(MW)~V plot (MW: molecular weight, V: elution volume) was obtained for the column and used to calculate the apparent molecular weight of BABZ proteins. The apparent MW divided by the calculated MW gave their aggregation states.

Isothermal titration calorimetry

An iTC200 Microcalorimeter (MicroCal, USA) was used to measure the binding affinities (K_d) between Zn^{2+} and BABZ proteins: 400 μmol/L BABZ protein dissolved in 100 mmol/L HEPES (pH 7.3), 50 mmol/L NaCl and 100 μmol/L TCEP was loaded into the cell, and 4 mmol/L $ZnSO_4$ in the same buffer was added automatically by syringe. The titration was performed at 25°C with an initial 0.4 μL injection in 0.8 s, followed by nineteen 2 μL injections in 4 s. The spacing between injections was 150 s, and the stirring speed during the titration was 1000 rpm. Data were collected every 5 s, and then analyzed using MicroCal Origin software by fitting to the single-site binding model. Correction for ligand dilution and other nonspecific interactions was carried out by performing a control experiment, using the same $ZnSO_4$ and HEPES buffers, and the heat effect was subtracted in the original data.

ACKNOWLEDGEMENTS

This work was supported in part by the Ministry of Science and Technology of China and the National Natural Science Foundation of China.

Supplementary material is available in the online version of this article at http://dx.doi.org/10.1007/s13238-011-1121-3 and is accessible for authorized users.

REFERENCES

Ambroggio, X.I., and Kuhlman, B. (2006). Computational design of a

single amino acid sequence that can switch between two distinct protein folds. J Am Chem Soc 128, 1154–1161.

Berg, J.M., and Shi, Y.G. (1996). The galvanization of biology: a growing appreciation for the roles of zinc. Science 271, 1081–1085.

Berman, H.M., Westbrook, J., Feng, Z., Gilliland, G., Bhat, T.N., Weissig, H., Shindyalov, I.N., and Bourne, P.E. (2000). The Protein Data Bank. Nucleic Acids Res 28, 235–242.

Cerasoli, E., Sharpe, B.K., and Woolfson, D.N. (2005). ZiCo: a peptide designed to switch folded state upon binding zinc. J Am Chem Soc 127, 15008–15009.

Choma, C.T., Lear, J.D., Nelson, M.J., Dutton, P.L., Robertson, D.E., and Degrado, W.F. (1994). DESIGN OF A HEME-BINDING 4-HELIX BUNDLE. J Am Chem Soc 116, 856–865.

Christianson, D.W., and Fierke, C.A. (1996). Carbonic anhydrase: Evolution of the zinc binding site by nature and by design. Acc Chem Res 29, 331–339.

Clarke, N.D., and Yuan, S.M. (1995). Metal search: a computer program that helps design tetrahedral metal-binding sites. Proteins 23, 256–263.

De Maeyer, M., Desmet, J., and Lasters, I. (1997). All in one: a highly detailed rotamer library improves both accuracy and speed in the modelling of sidechains by dead-end elimination. Fold Des 2, 53–66.

Dwyer, M.A., Looger, L.L., and Hellinga, H.W. (2003). Computational design of a Zn2 + receptor that controls bacterial gene expression. Proc Natl Acad Sci U S A 100, 11255–11260.

Dyer, R.B., Gai, F., and Woodruff, W.H. (1998). Infrared studies of fast events in protein folding. Acc Chem Res 31, 709–716.

Fry, H.C., Lehmann, A., Saven, J.G., DeGrado, W.F., and Therien, M. J. (2010). Computational design and elaboration of a de novo heterotetrameric alpha-helical protein that selectively binds an emissive abiological (porphinato)zinc chromophore. J Am Chem Soc 132, 3997–4005.

Handel, T.M., Williams, S.A., and DeGrado, W.F. (1993). Metal ion-dependent modulation of the dynamics of a designed protein. Science 261, 879–885.

Hellinga, H.W., and Richards, F.M. (1991). Construction of new ligand binding sites in proteins of known structure. I. Computer-aided modeling of sites with pre-defined geometry. J Mol Biol 222, 763–785.

Holm, R.H., Kennepohl, P., and Solomon, E.I. (1996). Structural and functional aspects of metal sites in biology. Chem Rev 96, 2239–2314.

Kaplan, J., and DeGrado, W.F. (2004). De novo design of catalytic proteins. Proc Natl Acad Sci U S A 101, 11566–11570.

Kiyokawa, T., Kanaori, K., Tajima, K., Koike, M., Mizuno, T., Oku, J.I., and Tanaka, T. (2004). Binding of Cu(II) or Zn(II) in a de novo designed triple-stranded alpha-helical coiled-coil toward a prototype for a metalloenzyme. J Pept Res 63, 347–353.

Li, W.F., Zhang, J., and Wang, W. (2007). Understanding the folding and stability of a zinc finger-based full sequence design protein with replica exchange molecular dynamics simulations. Proteins 67, 338–349.

Li, W.F., Zhang, J., Wang, J., and Wang, W. (2008). Metal-coupled folding of Cys2His2 zinc-finger. J Am Chem Soc 130, 892–900.

Liang, H.H., Chen, H., Fan, K.Q., Wei, P., Guo, X.R., Jin, C.W., Zeng, C., Tang, C., and Lai, L.H. (2009). De novo design of a beta alpha beta motif. Angew Chem Int Ed Engl 48, 3301–3303.

Lombardi, A., Summa, C.M., Geremia, S., Randaccio, L., Pavone, V., and DeGrado, W.F. (2000). Retrostructural analysis of metalloproteins: application to the design of a minimal model for diiron proteins. Proc Natl Acad Sci U S A 97, 6298–6305.

Lu, Y., Berry, S.M., and Pfister, T.D. (2001). Engineering novel metalloproteins: design of metal-binding sites into native protein scaffolds. Chem Rev 101, 3047–3080.

Lu, Y., Yeung, N., Sieracki, N., and Marshall, N.M. (2009). Design of functional metalloproteins. Nature 460, 855–862.

Matzapetakis, M., Farrer, B.T., Weng, T.C., Hemmingsen, L., Penner-Hahn, J.E., and Pecoraro, V.L. (2002). Comparison of the binding of cadmium(II), mercury(II), and arsenic(III) to the de novo designed peptides TRI L12C and TRI L16C. J Am Chem Soc 124, 8042–8054.

Meinnel, T., Blanquet, S., and Dardel, F. (1996). A new subclass of the zinc metalloproteases superfamily revealed by the solution structure of peptide deformylase. J Mol Biol 262, 375–386.

Miller, J.C., Holmes, M.C., Wang, J.B., Guschin, D.Y., Lee, Y.L., Rupniewski, I., Beausejour, C.M., Waite, A.J., Wang, N.S., Kim, K. A., *et al.* (2007). An improved zinc-finger nuclease architecture for highly specific genome editing. Nat Biotechnol 25, 778–785.

Müller, H.N., and Skerra, A. (1994). Grafting of a high-affinity Zn(II)-binding site on the beta-barrel of retinol-binding protein results in enhanced folding stability and enables simplified purification. Biochemistry 33, 14126–14135.

Nomura, A., and Sugiura, Y. (2004). Hydrolytic reaction by zinc finger mutant peptides: successful redesign of structural zinc sites into catalytic zinc sites. Inorg Chem 43, 1708–1713.

Pasquinelli, R.S., Shepherd, R.E., Koepsel, R.R., Zhao, A., and Ataai, M.M. (2000). Design of affinity tags for one-step protein purification from immobilized zinc columns. Biotechnol Prog 16, 86–91.

Petros, A.K., Reddi, A.R., Kennedy, M.L., Hyslop, A.G., and Gibney, B.R. (2006). Femtomolar Zn(II) affinity in a peptide-based ligand designed to model thiolate-rich metalloprotein active sites. Inorg Chem 45, 9941–9958.

Phillips, N.B., Wan, Z.L., Whittaker, L., Hu, S.Q., Huang, K., Hua, Q. X., Whittaker, J., Ismail-Beigi, F., and Weiss, M.A. (2010). Supramolecular protein engineering: design of zinc-stapled insulin hexamers as a long acting depot. J Biol Chem 285, 11755–11759.

Proudfoot, C., McPherson, A.L., Kolb, A.F., and Stark, W.M. (2011). Zinc finger recombinases with adaptable DNA sequence specificity. PLoS One 6, e19537.

Reddi, A.R., Guzman, T.R., Breece, R.M., Tiemey, D.L. and Gibney, B.R. (2007). Deducing the Energetic Cost of Protein Folding in Zinc Finger Proteins Using Designed Metallopeptides. J Am Chem Soc, 129, 12815–12827.

Regan, L., and Clarke, N.D. (1990). A tetrahedral zinc(II)-binding site introduced into a designed protein. Biochemistry 29, 10878–10883.

Shults, M.D., Pearce, D.A., and Imperiali, B. (2003). Modular and tunable chemosensor scaffold for divalent zinc. J Am Chem Soc 125, 10591–10597.

Smith, B.A., and Hecht, M.H. (2011). Novel proteins: from fold to function. Curr Opin Chem Biol 15, 421–426.

Stevens, F.J. (1986). Analysis of protein-protein interaction by

simulation of small-zone size-exclusion chromatography: application to an antibody-antigen association. Biochemistry 25, 981–993.

Wade, W.S., Koh, J.S., Han, N., Hoekstra, D.M., and Lerner, R.A. (1993). Engineering Metal Coordination Sites into the Antibody Light-Chain. J Am Chem Soc 115, 4449–4456.

Winzor, D.J. (2003). Analytical exclusion chromatography. J Biochem Biophys Methods 56, 15–52.

Wu, J., Kandavelou, K., and Chandrasegaran, S. (2007). Custom-designed zinc finger nucleases: what is next? Cell Mol Life Sci 64, 2933–2944.

